

May 19-23, 2014

# Hands-on Workshop on Computational Biophysics

by

The Theoretical and Computational Biophysics Group  
(**TCBG**)

and

The National Center for Multiscale Modeling of  
Biological Systems (**MMBioS**)

# Workshop Program

**Thu, May 22: Collective Dynamics of Proteins Using Elastic Network Models -**

*Bahar, Tim Lezon and Chakra Chennubhotla*

**Fri, May 23: Druggability Simulations, and Analyzing Sequence Patterns and Structural Dynamics -** *Ivet Bahar , Indira Shrivastava, Chakra Chennubhotla,*

# Druggable Genome

A small subset of are 'disease-modifying' – and not all of them are druggable

Human Genome (21,000) genes

The diagram consists of a large teal oval representing the Human Genome (21,000 genes). Inside this oval are two overlapping ovals: an orange one on the left representing the Druggable genome (3,000 genes) and a green one on the right representing Disease-related genes (~3,000 genes). The intersection of these two ovals is a yellow oval representing Drug Targets (600-1,500). The Drug Targets oval also lists 70+ kinases and 100+ GPCRs. The Druggable genome oval lists 430+ kinases and 600+ GPCRs.

Druggable genome  
3,000 genes

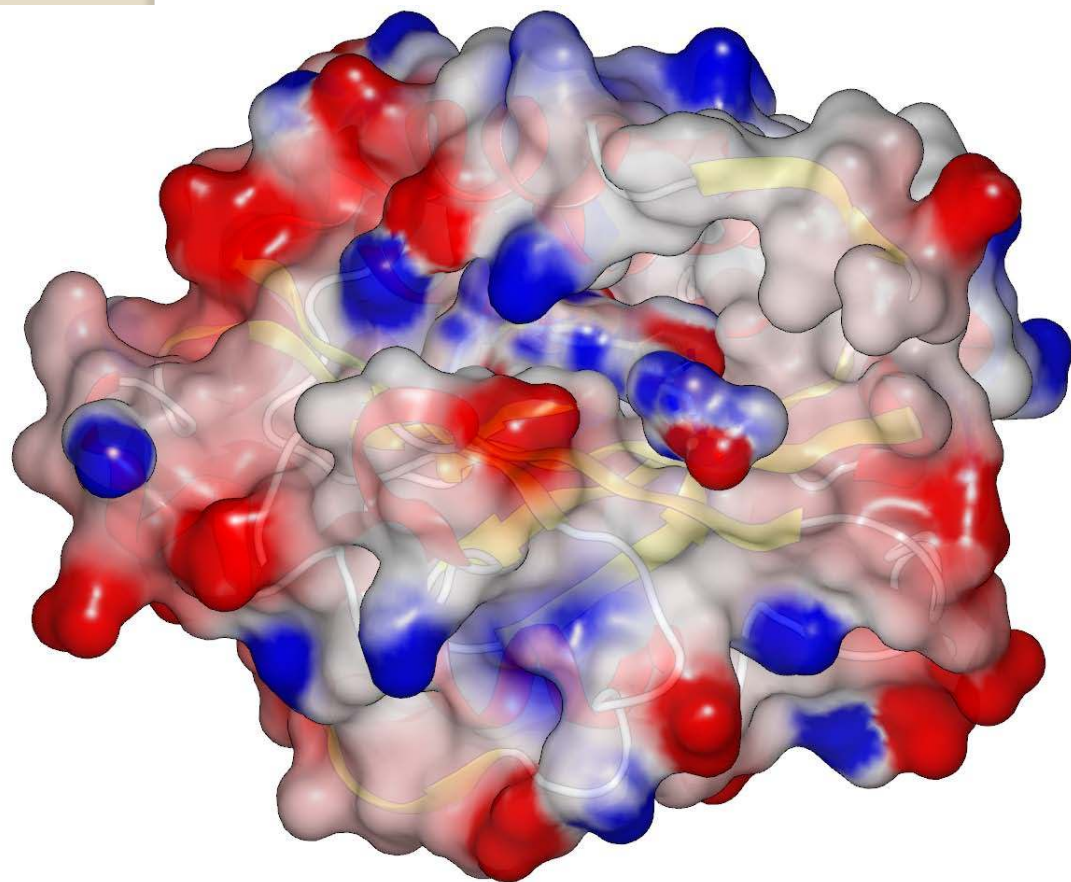
430+ kinases  
600+ GPCRs

70+ kinases  
100+ GPCRs

**Drug  
Targets**  
600-1,500

Disease-related genes  
~3,000 genes

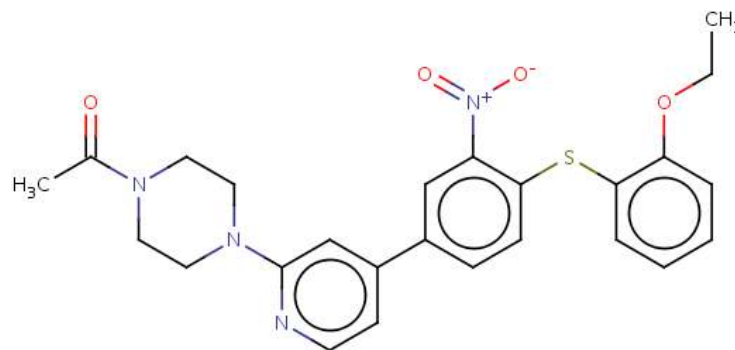
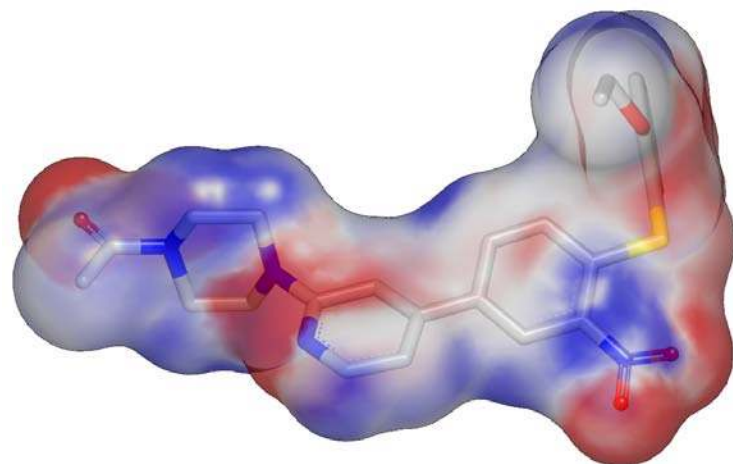
# Druggable or not?



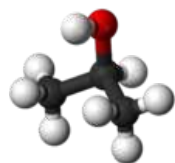
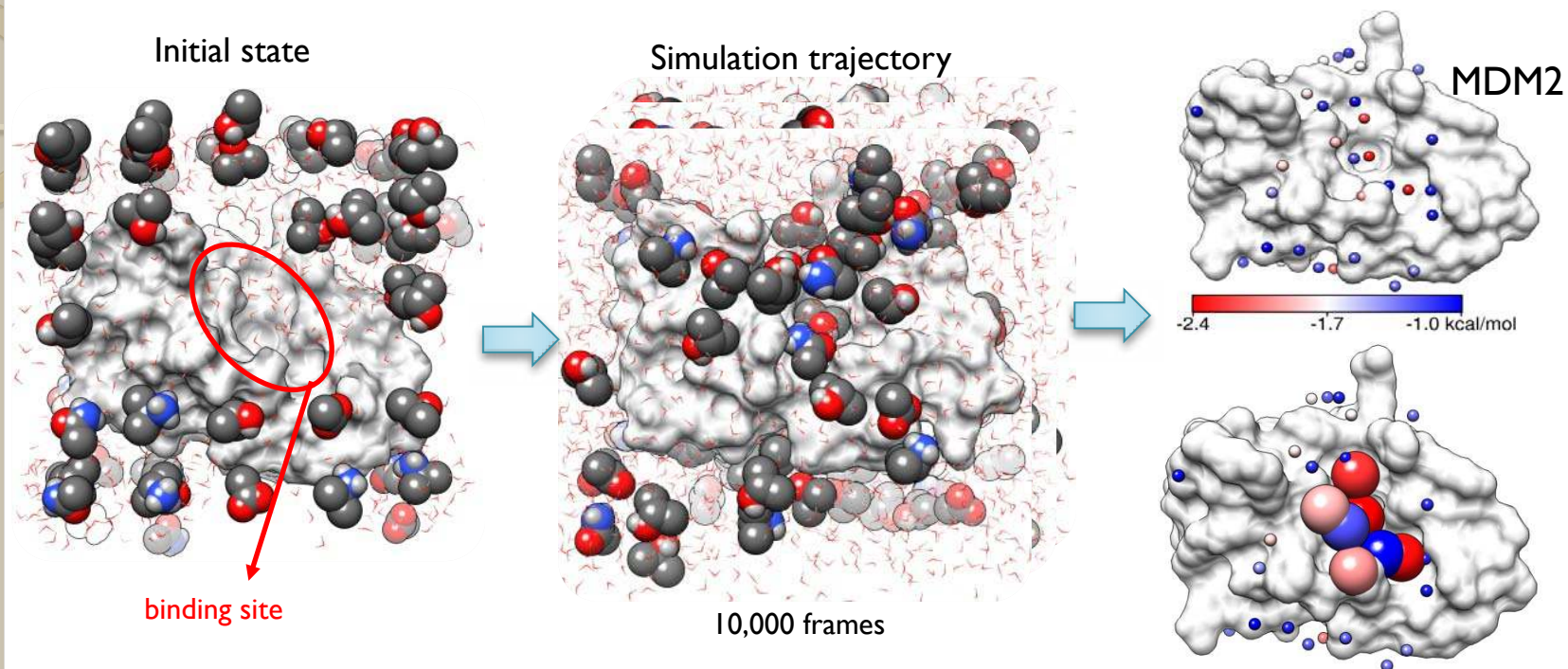
**Lfa1** - a leukocyte glycoprotein that promotes intercellular adhesion and binds intercellular adhesion molecule 1

## Active site druggability:

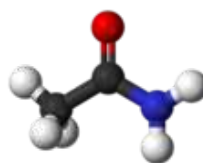
- Best known  $K_d$  18.3 nM
- Simulation 0.03-0.5 nM



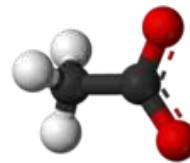
# Druggability Simulations



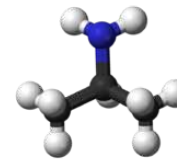
Isopropanol  
(observed in 57% of drugs)



Acetamide  
(21%)

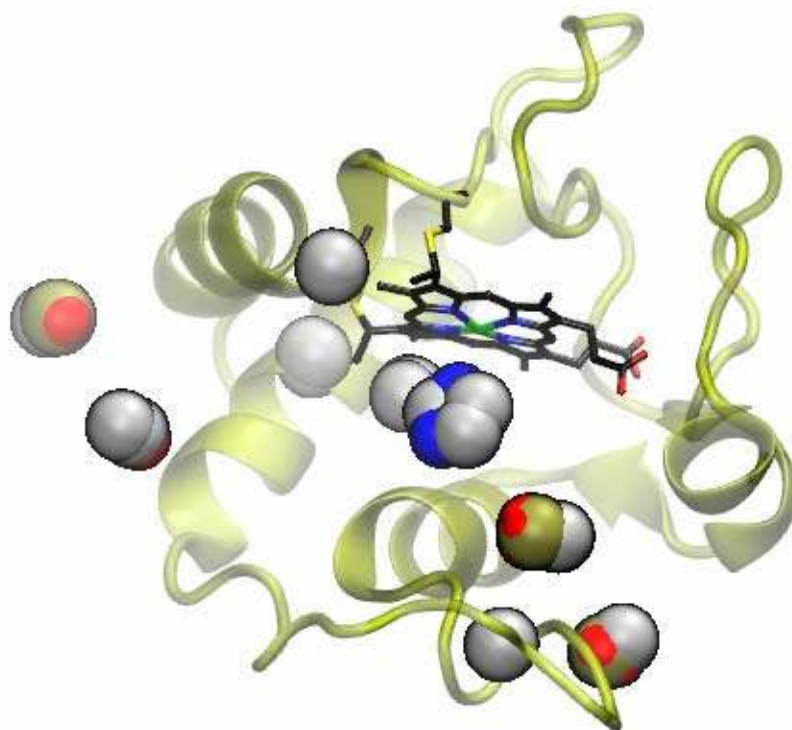


Acetate (-1)  
(21%)



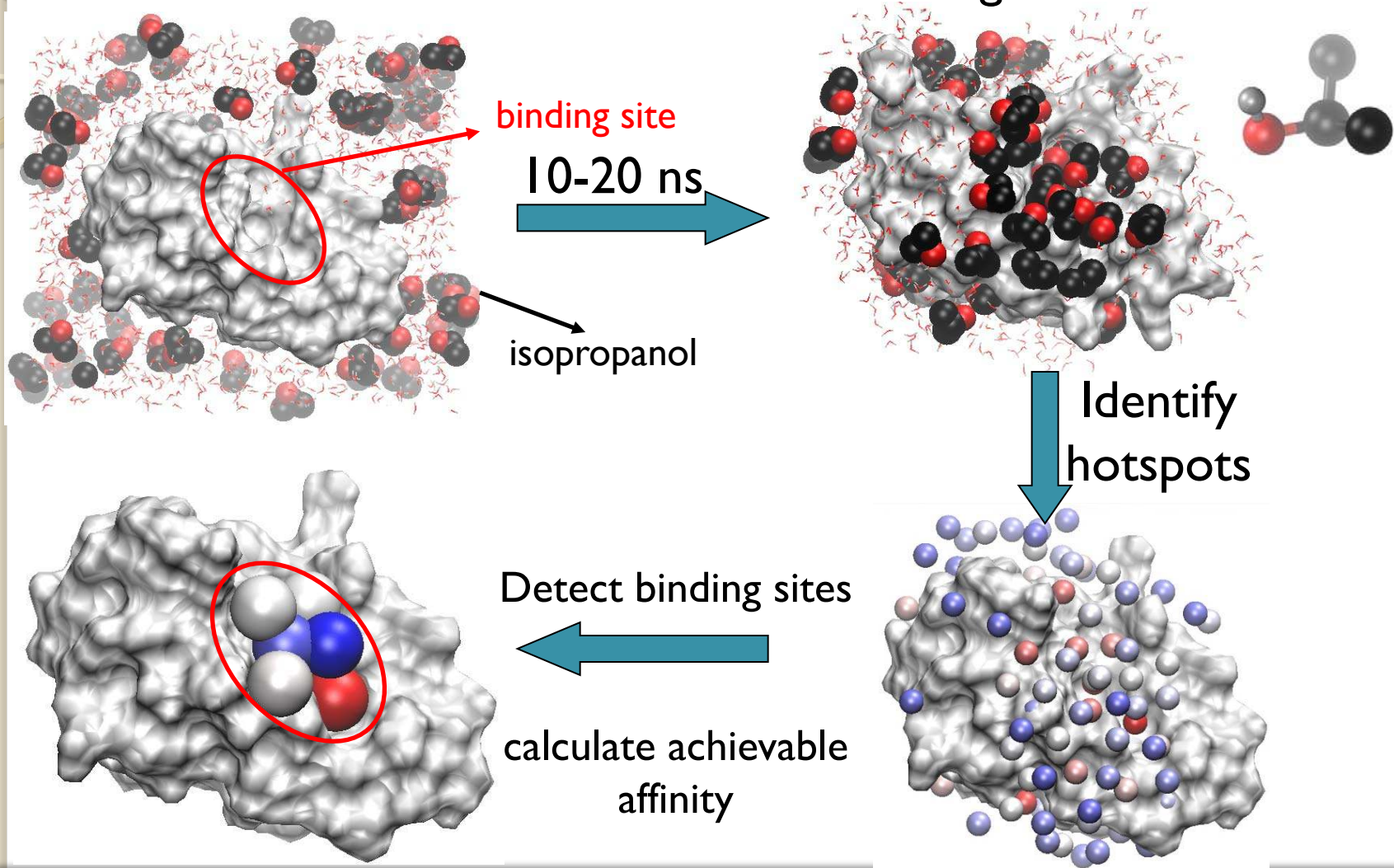
Isopropylamine (+1)  
(25%)

# Cytochrome c druggability

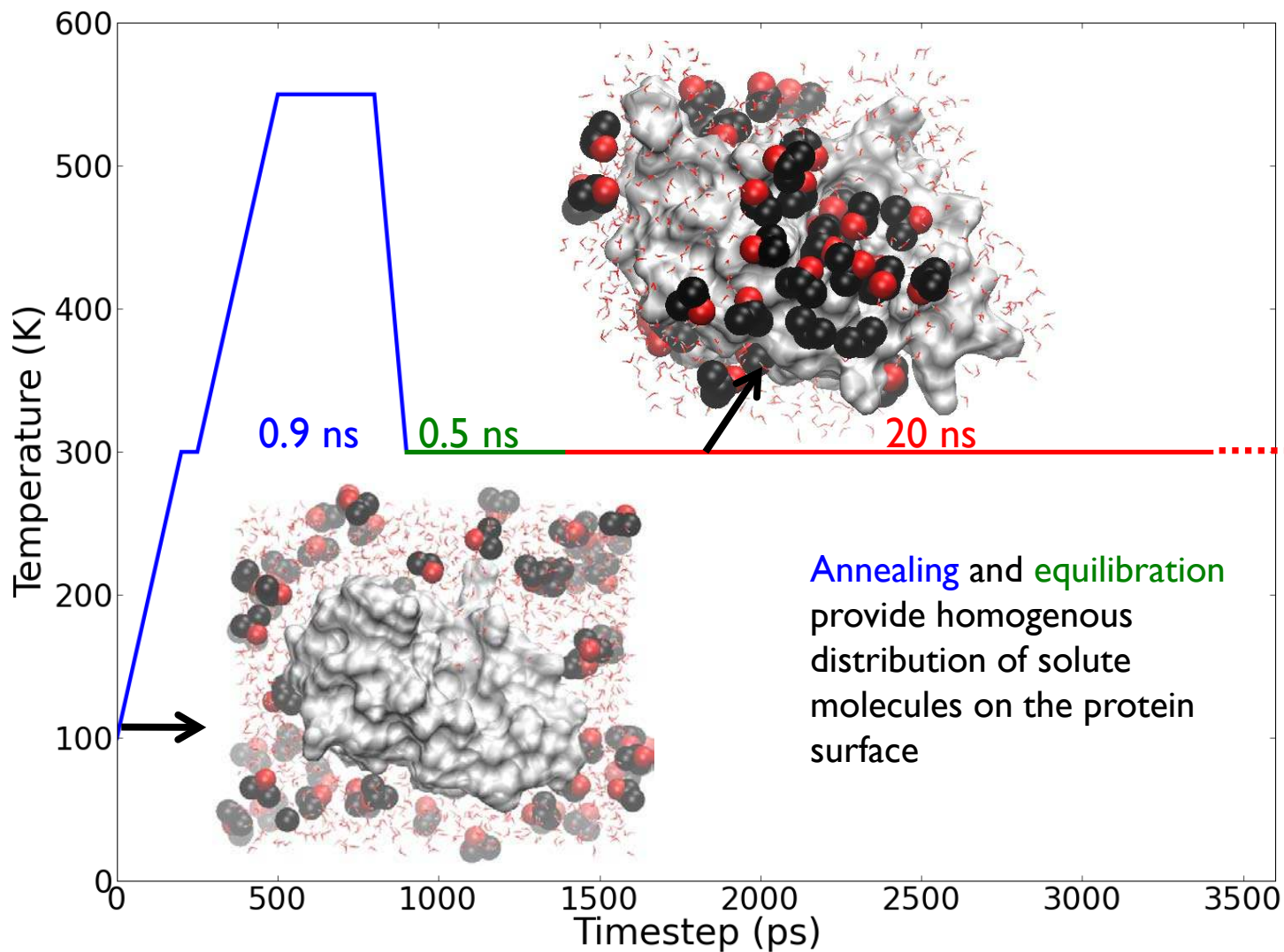


# Methodology Overview

From MD simulations to achievable drug affinities



# Annealing, Equilibration, Simulation

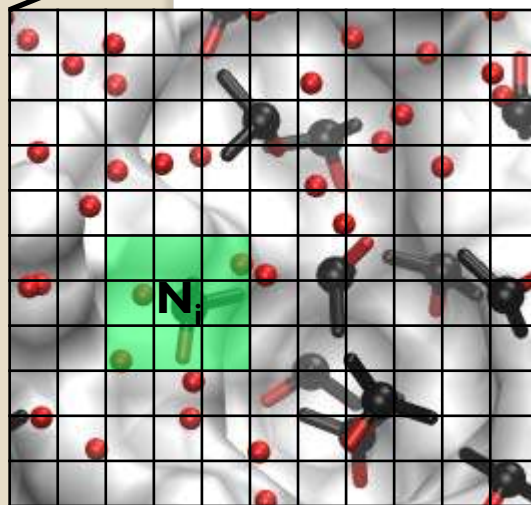
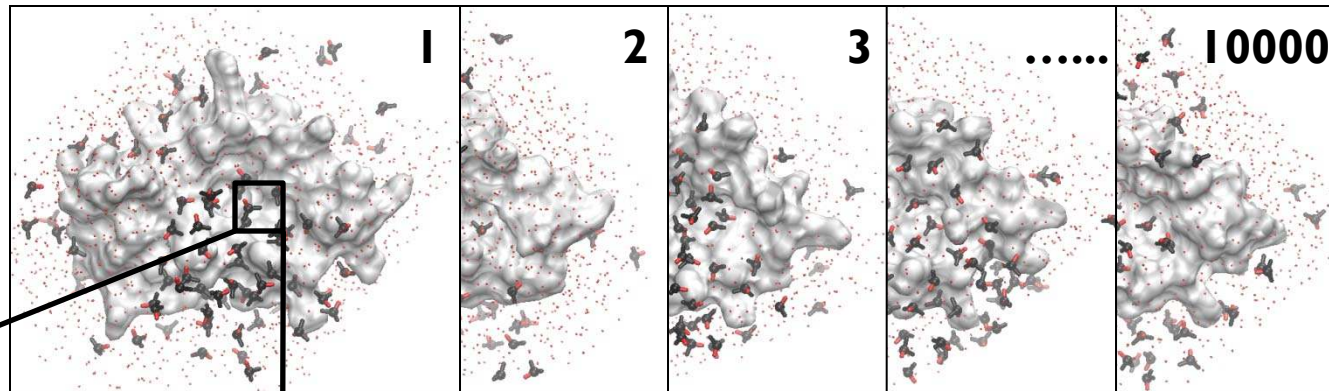


NAMD2 with CHARMM force field was used for simulations.



# Free Energy of Binding for Isopropanol

Assuming that MD sampling converged to a **Boltzmann ensemble**

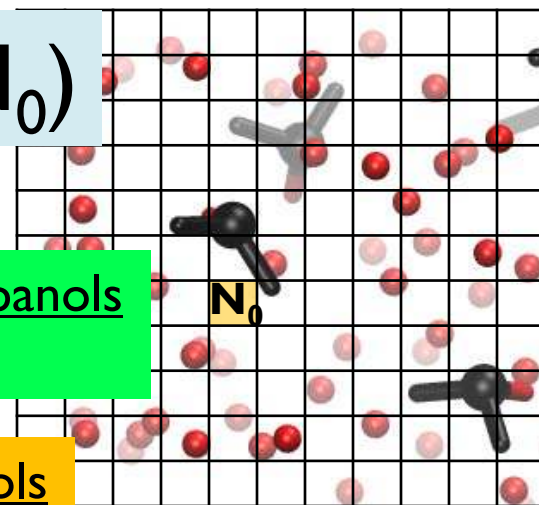


0.5 Å (not to scale)

$$\Delta G_i = -RT \ln(N_i/N_0)$$

$N_i$  = observed number of isopropanols  
(# of frames) \* (# of cubes)

$N_0$  = total number of isopropanols  
total number of frames



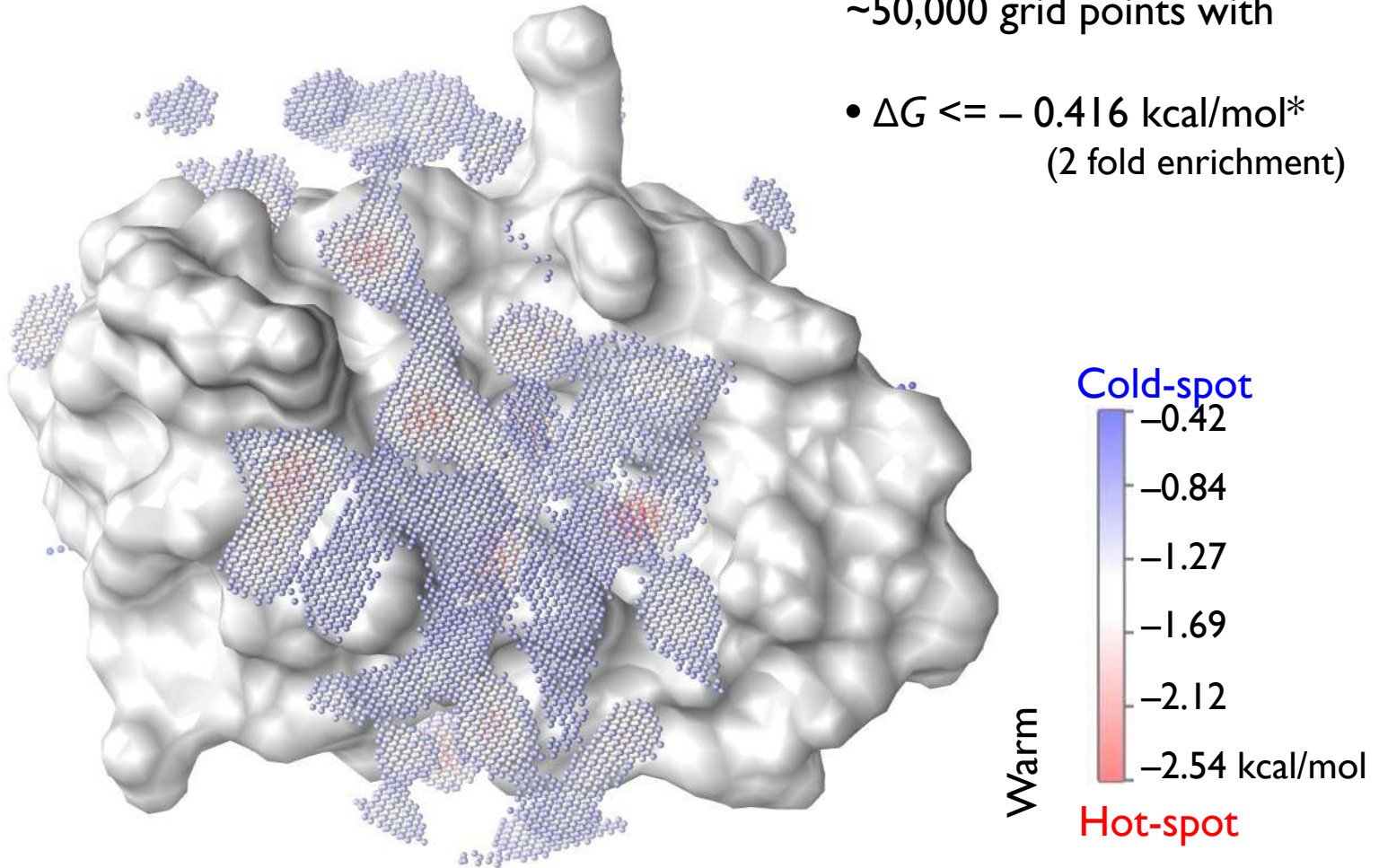
$N_i$  corresponds to the central highlighted grid element;  
number of cubes is introduced if multiple cubes are occupied by a single isopropanol

# Isopropanol Binding Spots

$\Delta G$  grid is mapped onto the protein structure

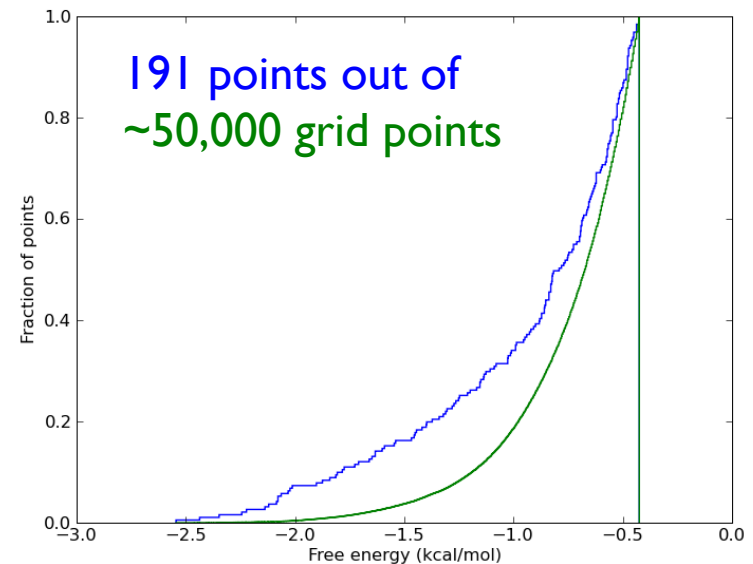
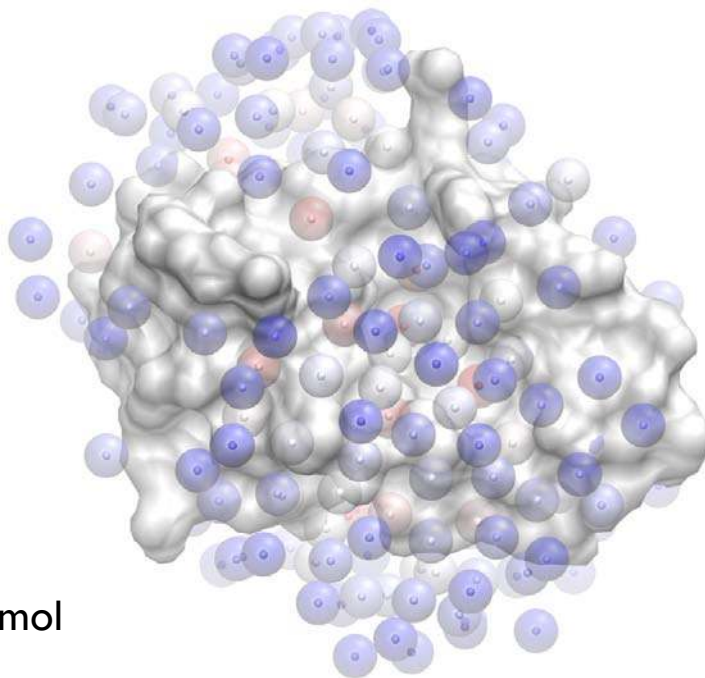
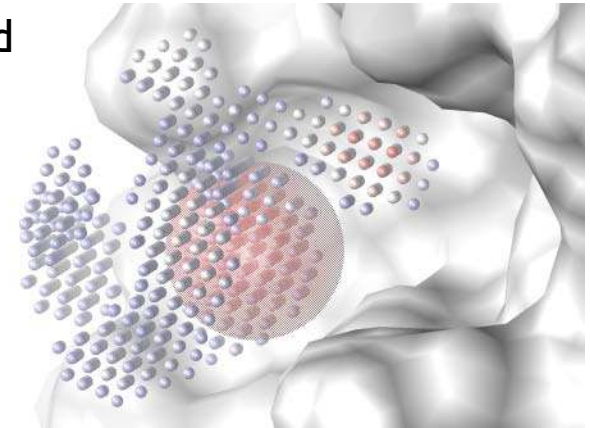
~50,000 grid points with

- $\Delta G \leq -0.416$  kcal/mol\*  
(2 fold enrichment)



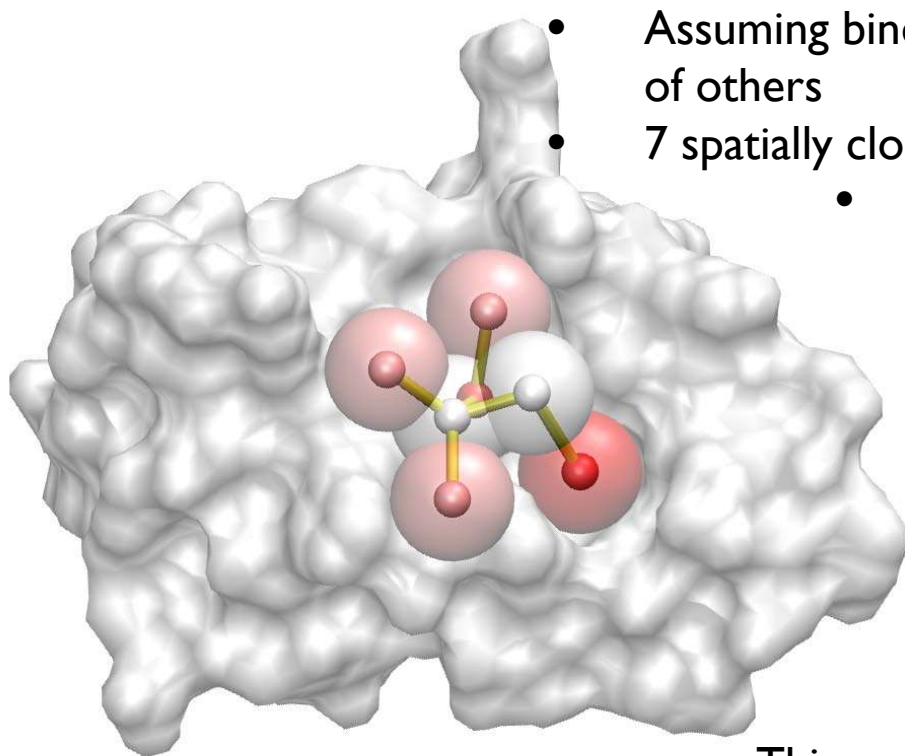
# Selecting Isopropanol Binding Spots

1. Grid element with lowest  $\Delta G$  value is selected
2. Other elements within **4 Å** are removed (elements inside the red sphere  $\rightarrow$ )
3. 1 and 2 are repeated until no more points are left to remove



# Affinity of a Drug-size Molecule

A heuristic approach for calculating achievable free energy of binding



- Assuming binding of an isopropanol is independent of others

- 7 spatially close binding spots are selected

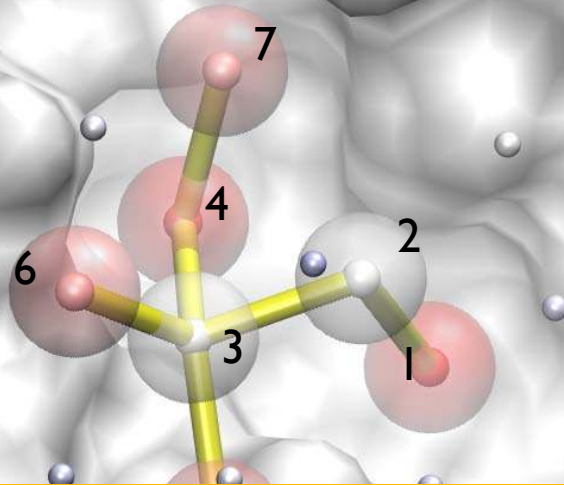
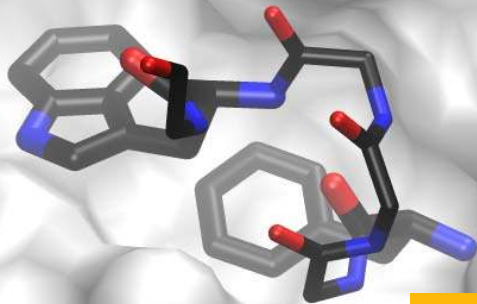
- The sum of  $\Delta G_{binding}$  of individual points is considered as a binding free energy estimate that is achievable by a drug-like molecule

This way, the highest affinity we can observe is 5 fM ( $10^{-15}$ ).

# MDM2: p53 binding site

p53 peptide key interactions (X-ray)

Highest affinity solution (7 points)



The top solution is in the protein-protein interaction site

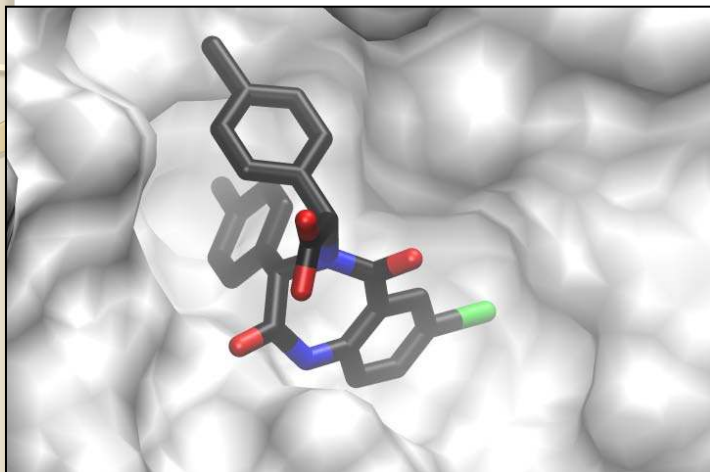
Numbers indicate the order that hot spots were merged by the growing algorithm

Predicted binding affinity range : **0.05-0.3 nM**

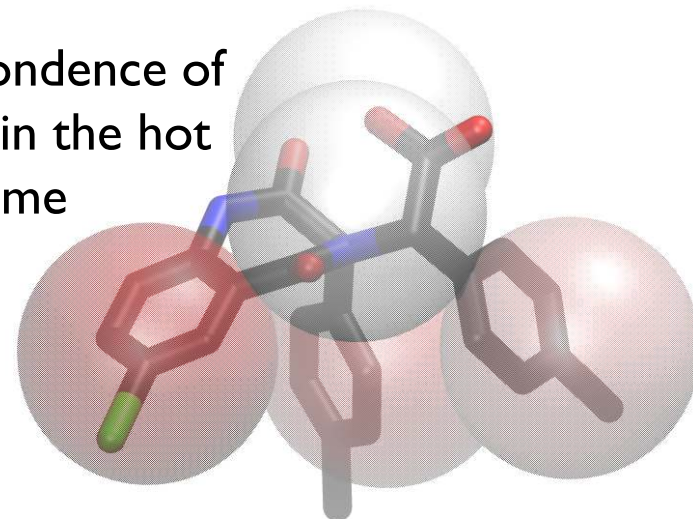
Predicted max. affinity by Seco et al. : **0.02 nM**

# MDM2: p53 binding site

An inhibitor that disrupts p53 binding

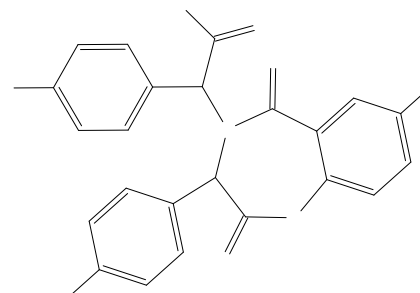
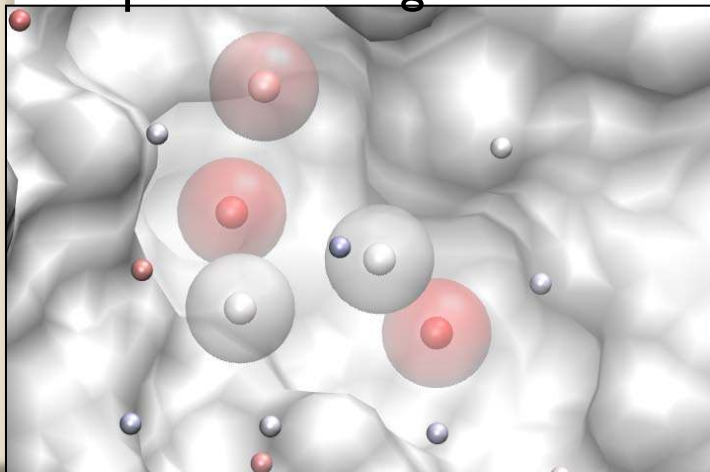


Correspondence of inhibitor in the hot spot volume



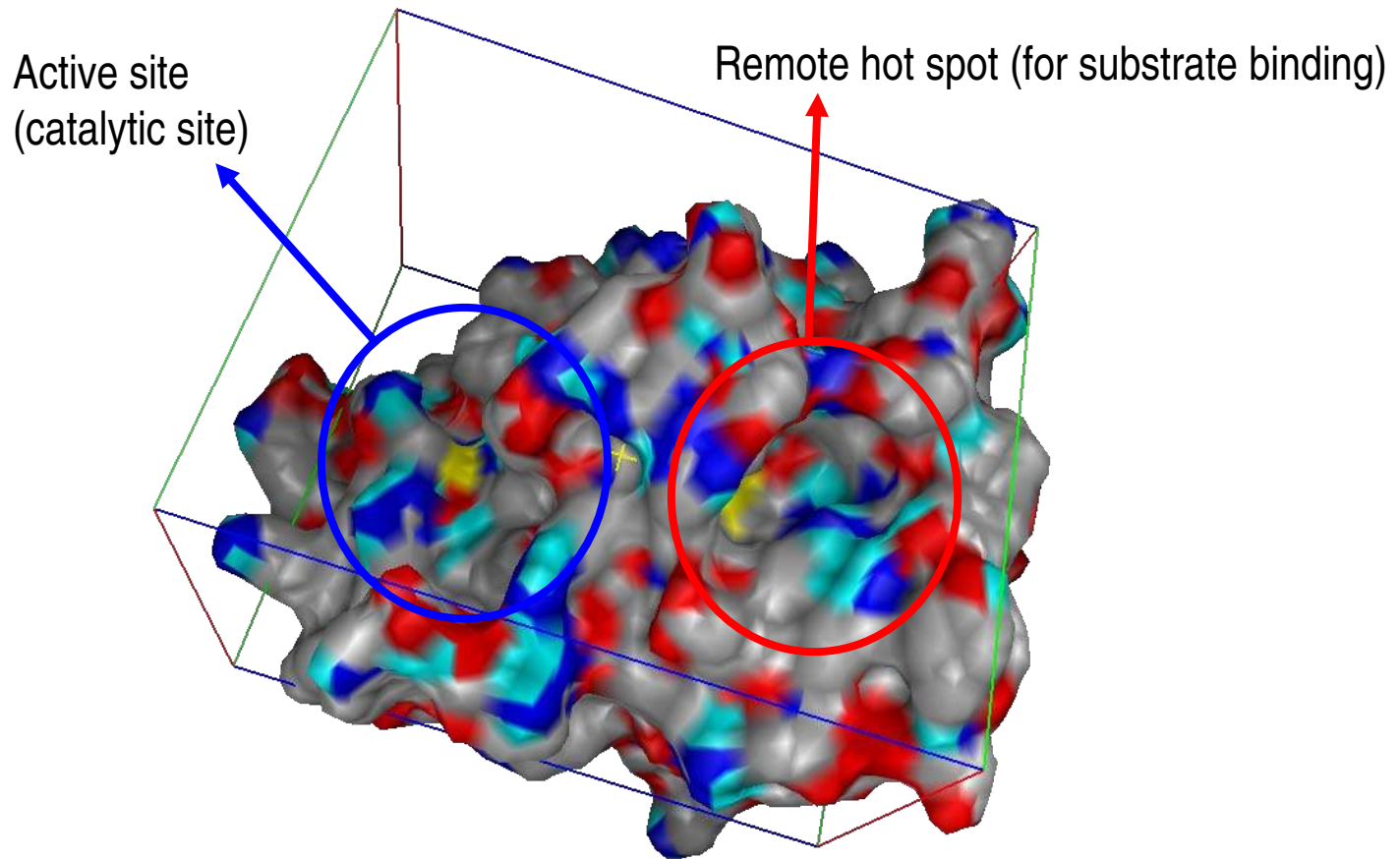
Predicted  $K_d$ : **47 nM**  
Known  $K_d$  : **80 nM**

Hot spots matching this inhibitor

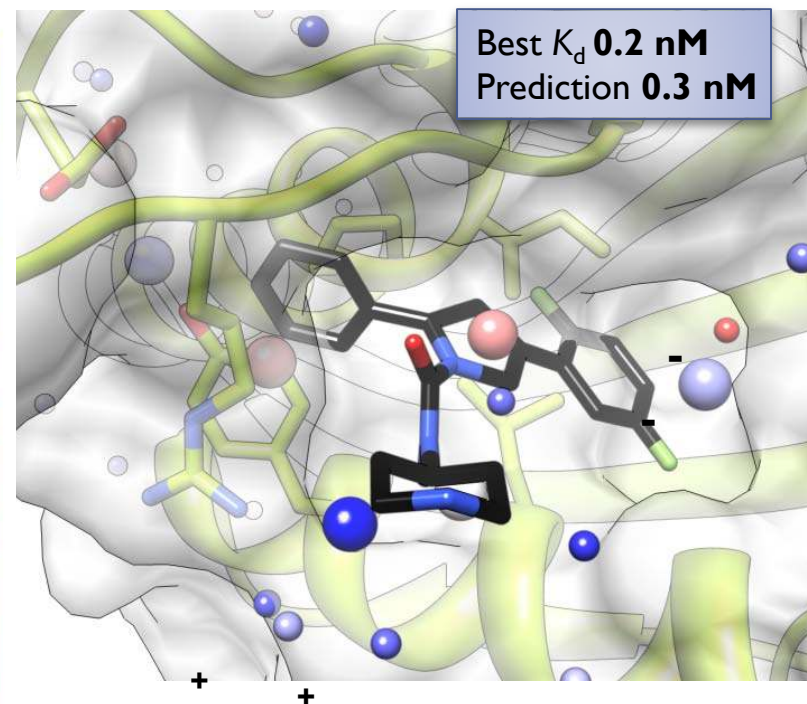
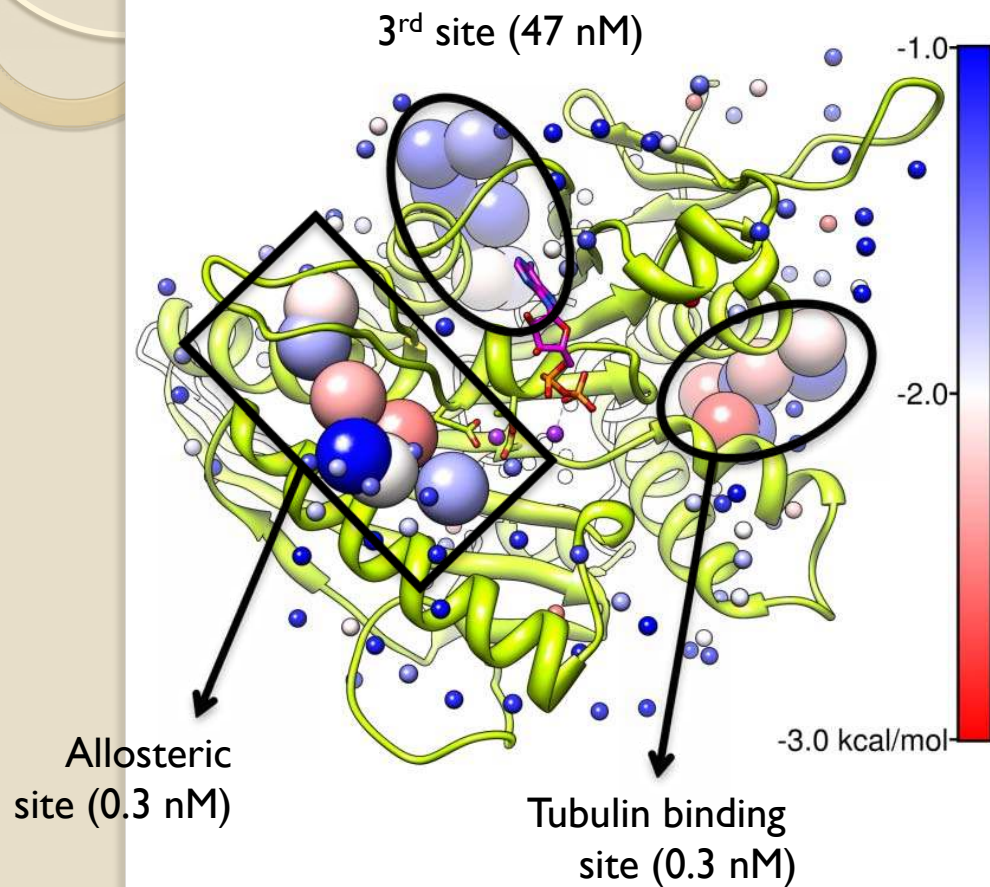


HAC = 32  
MW = 580

# Proteins may have multiple target sites



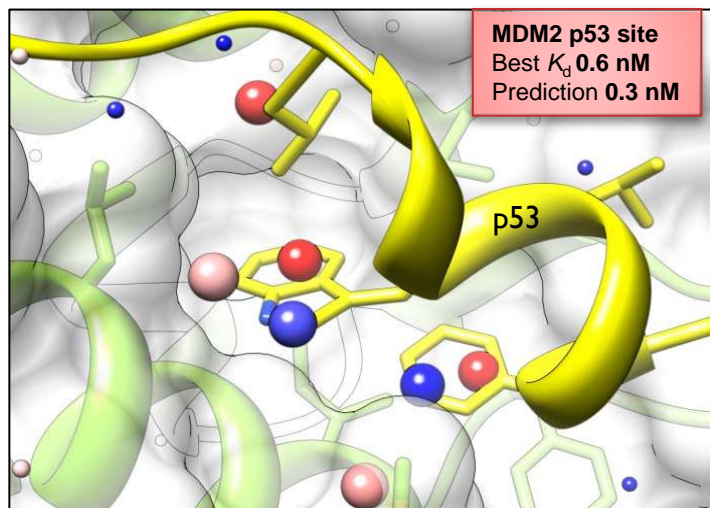
# eg5 Druggable Sites



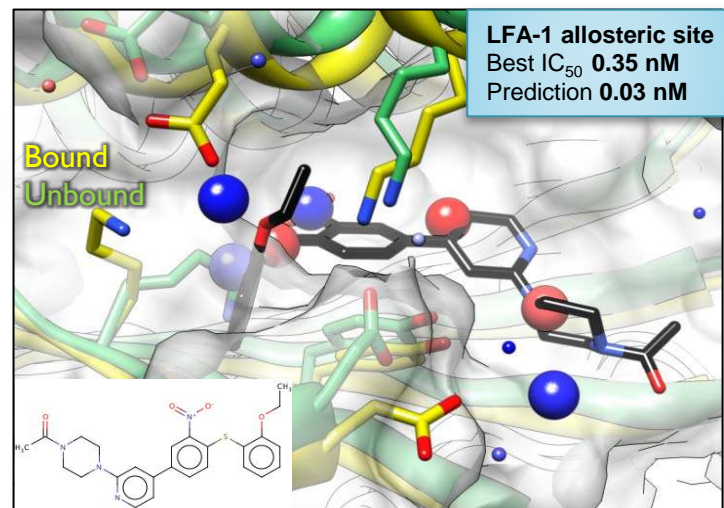
*Bioorg. Med. Chem. Lett.* **2007**, *17*, 5677-5682



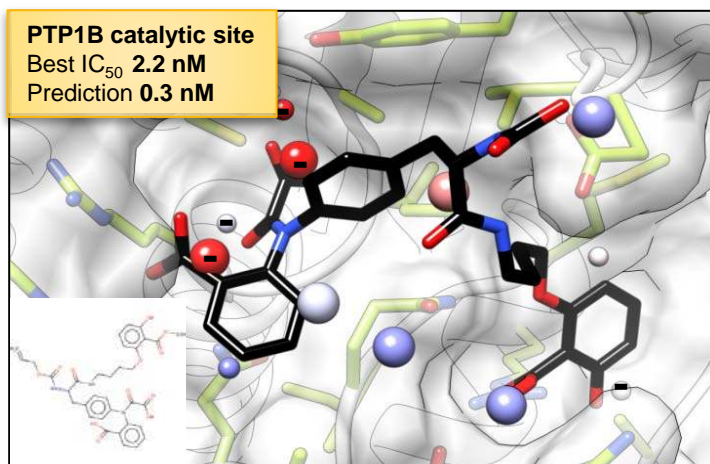
# Assessment of druggable allosteric sites



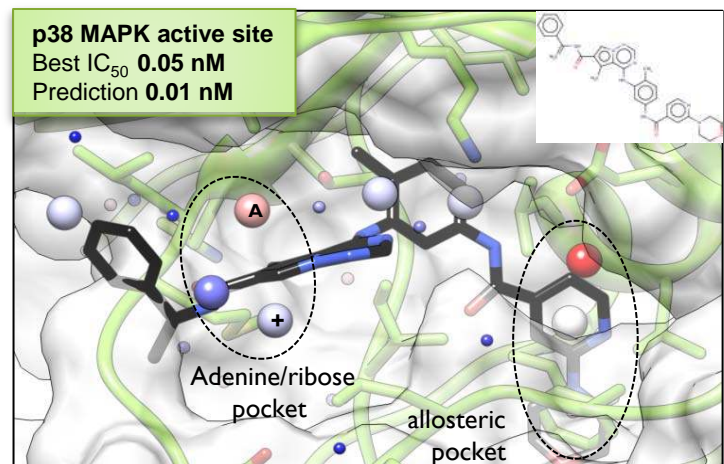
*J Med. Chem.* **2009**, 52, 7970-7973



*Biochemistry* **2004**, 43, 2394-2404



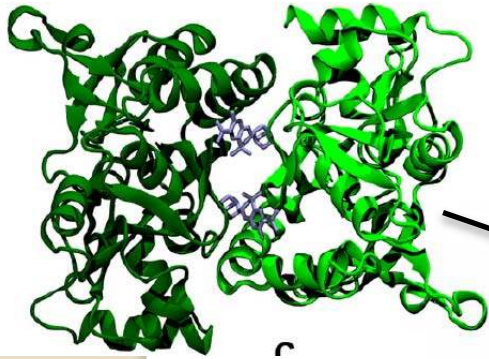
*Bioorg. Med. Chem. Lett.* **2003**, 13, 3947-3950



*J Med. Chem.* **2010**, 53, 2973-2985

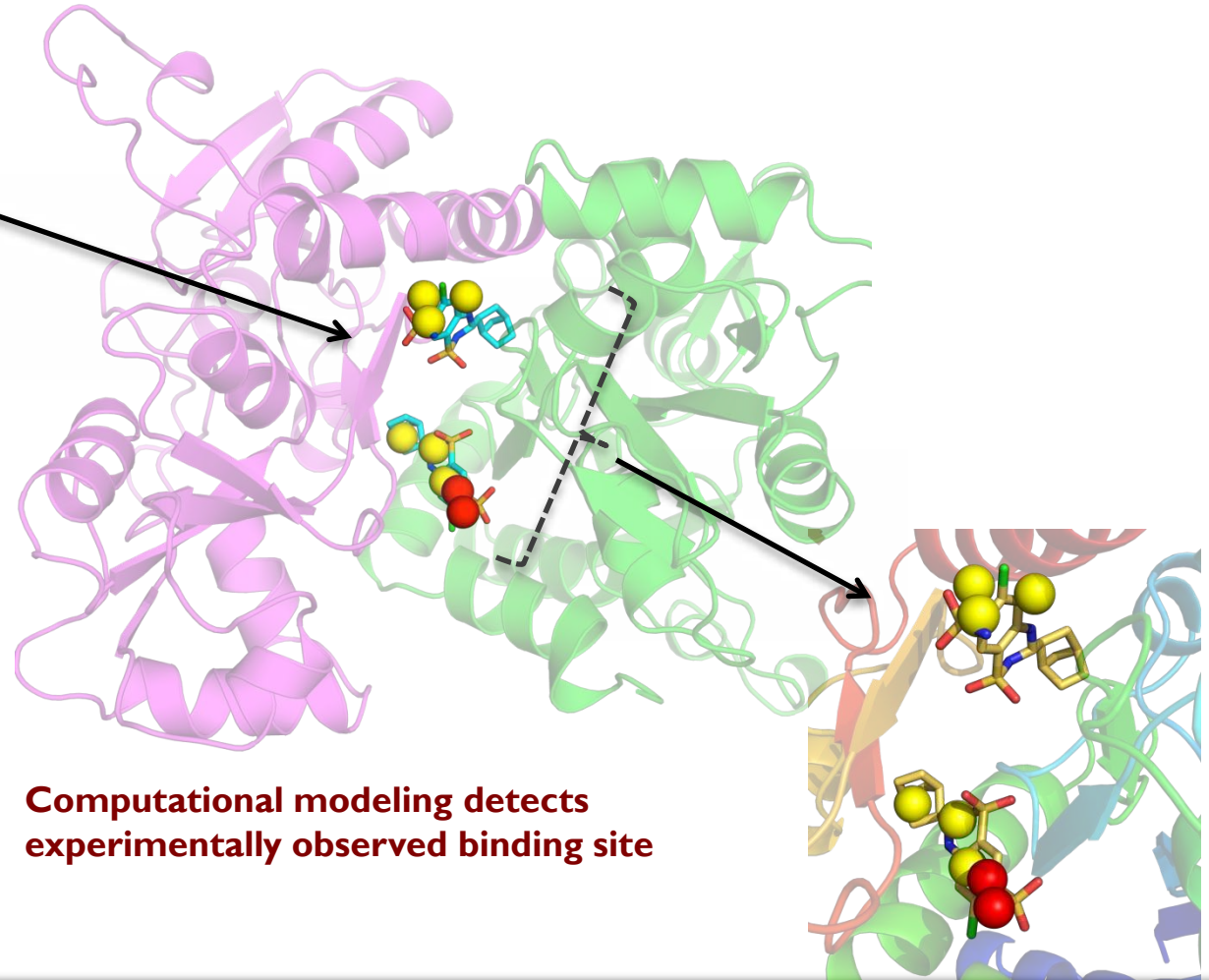
## 2

# Probes capture allosteric modulator site of AMPAR LBD Dimer



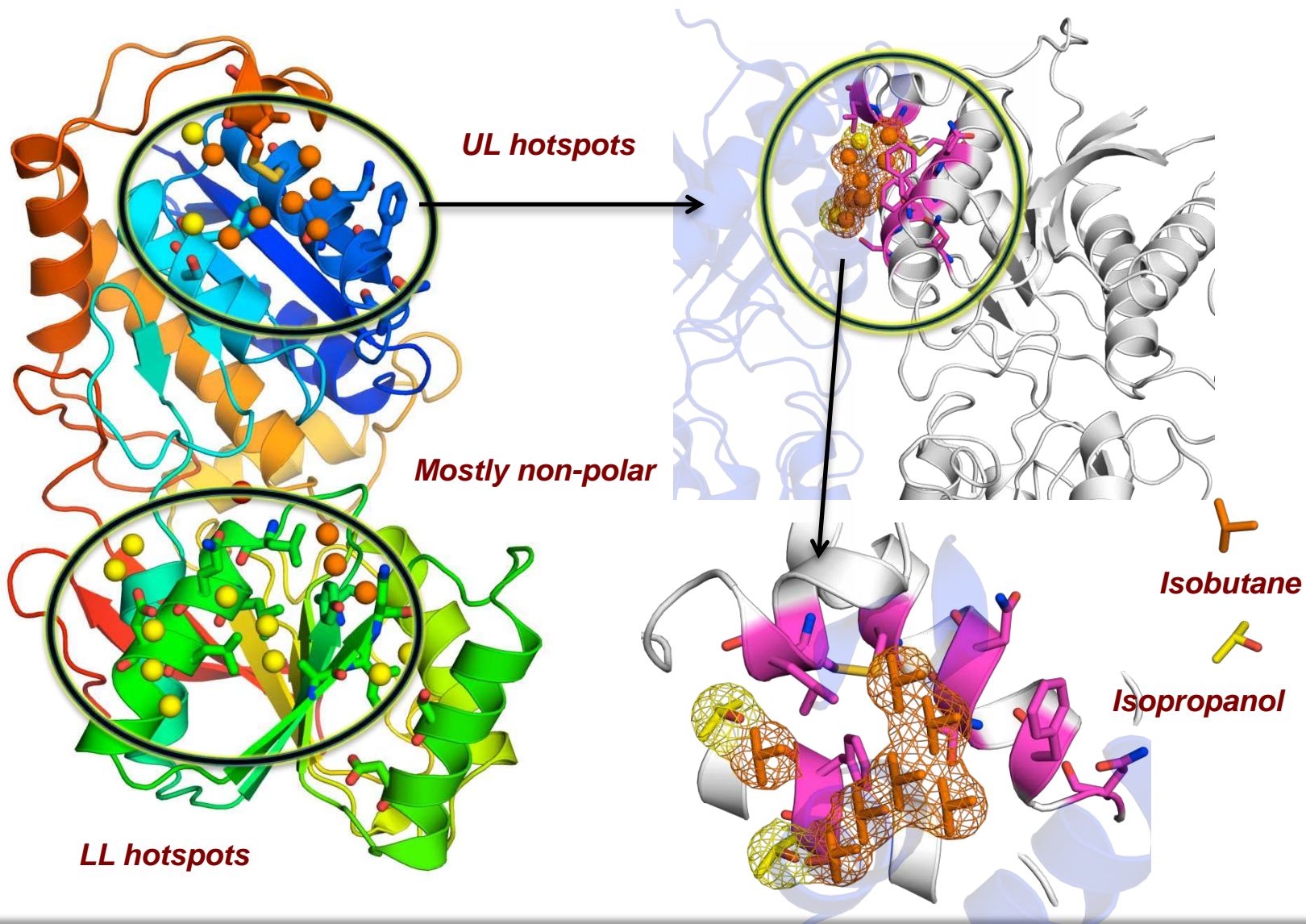
## Experimental Results

Pohlsгарrd et al (2011).  
Neuropharmacology. 60,135-150.



**Computational modeling detects  
experimentally observed binding site**

# Interfacial regions captured in AMPAR NTD

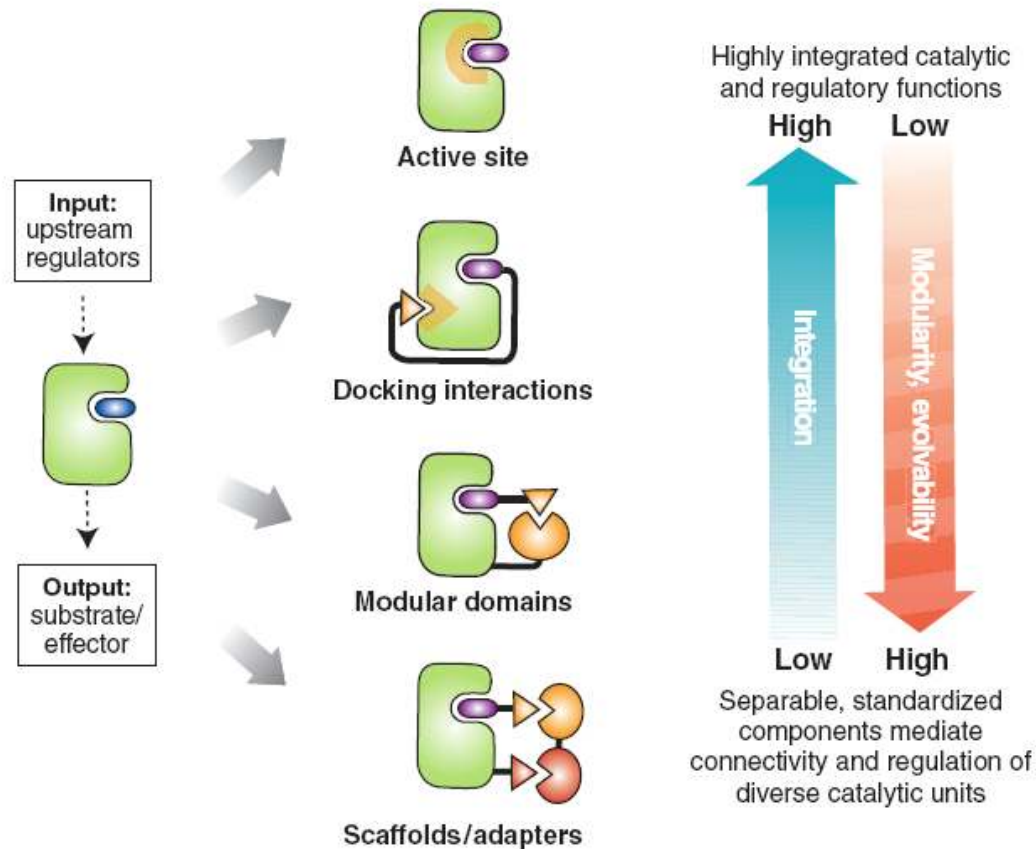




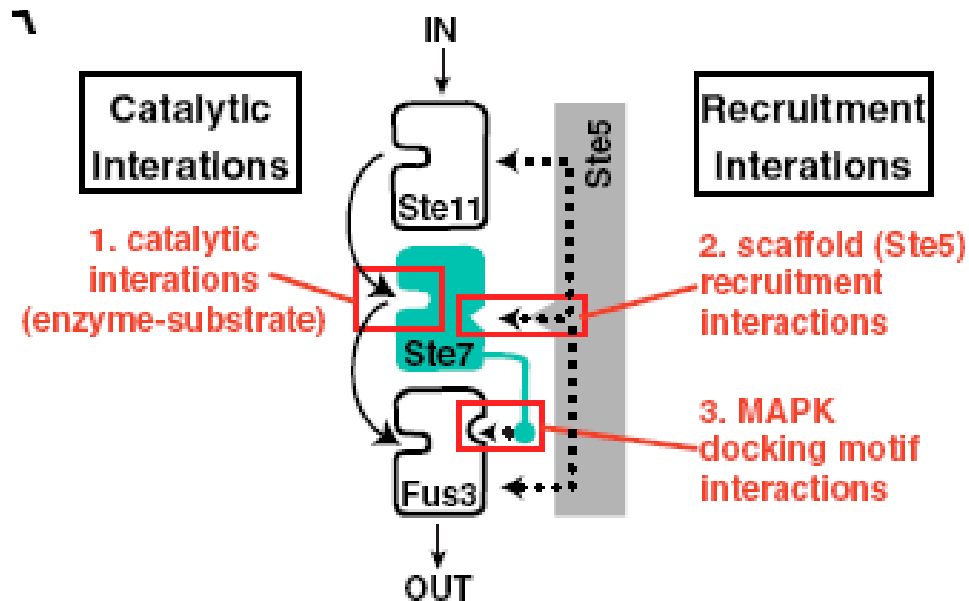
# SUMMARY

- 1 ● Structure-encoded **flexibility** of drug targets and significance in drug discovery and design
- 2 ● **Druggability** assessment: a first step before selecting a target
- 3 ● Modularity and **promiscuity** of proteins and **quantitative systems pharmacology** methods

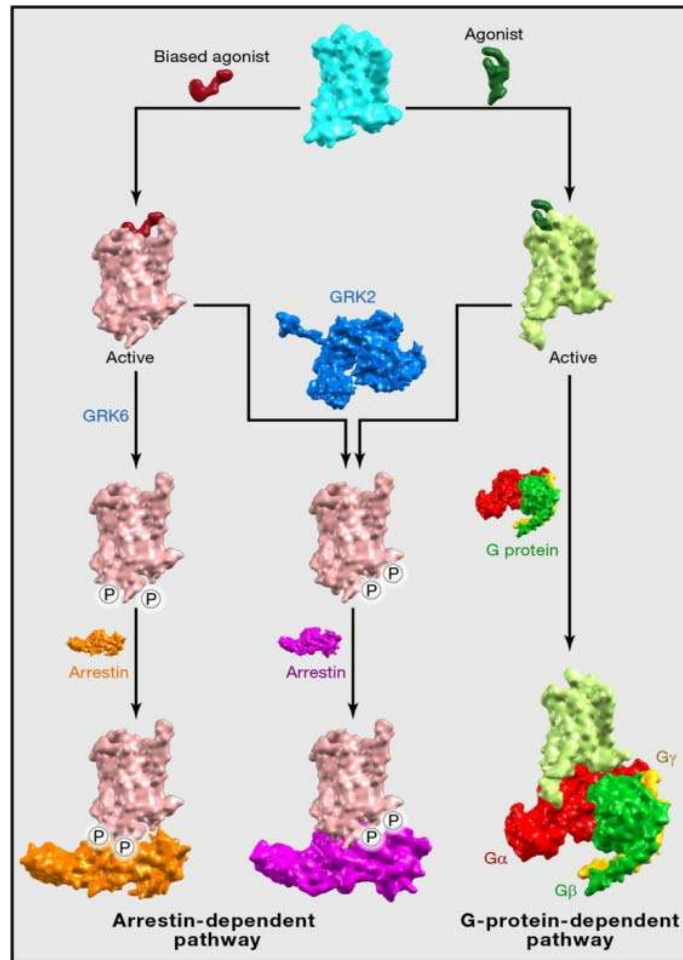
# Diversity & complexity of phenotypes arise from combinations of proteins & modular domains



# Significance of targeting a specific site, not only a target protein



# Allostery Can Diversify Cellular Signaling Pathways through a Single Receptor



GPCRs use **conformational selection** to shape signaling.

Two (different) conformations of GPCR bind two (different) agonists, which branch into two pathways

# Protein Promiscuity

Many proteins are involved in multiple pathways.

Depending on the targeted **surface** region, or on the accessible **structural change/dynamics**

the interactions with different (or multiple) upstream or downstream partners/substrates may be affected,

which in turn would impact different (or multiple) pathways, and may result in various phenotypes

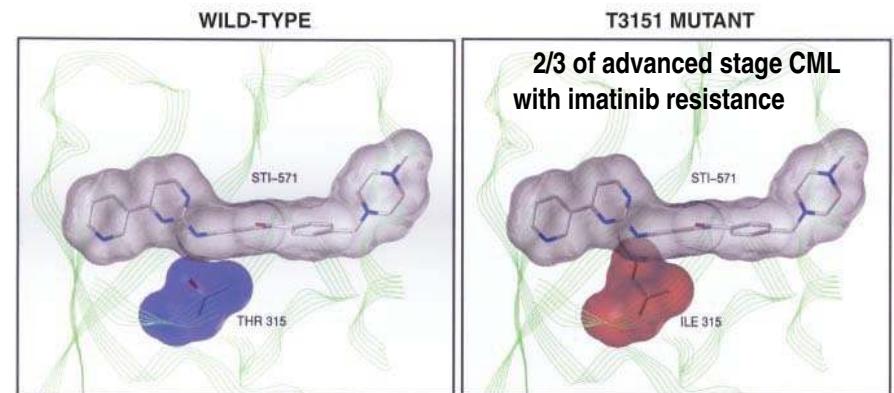
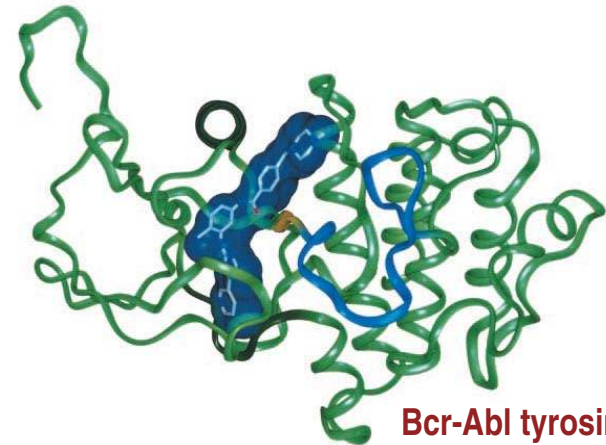


# Assessment of druggable allosteric sites

## Imatinib (Gleevec)

**TIME**  
 THERE IS NEW **AMMUNITION**  
 IN THE WAR AGAINST  
**CANCER.**  
**THESE ARE THE BULLETS.**  
 Revolutionary new pills like **GLEEVEC**  
 combat cancer by targeting only the  
 diseased cells. Is this the breakthrough  
 we've been waiting for?

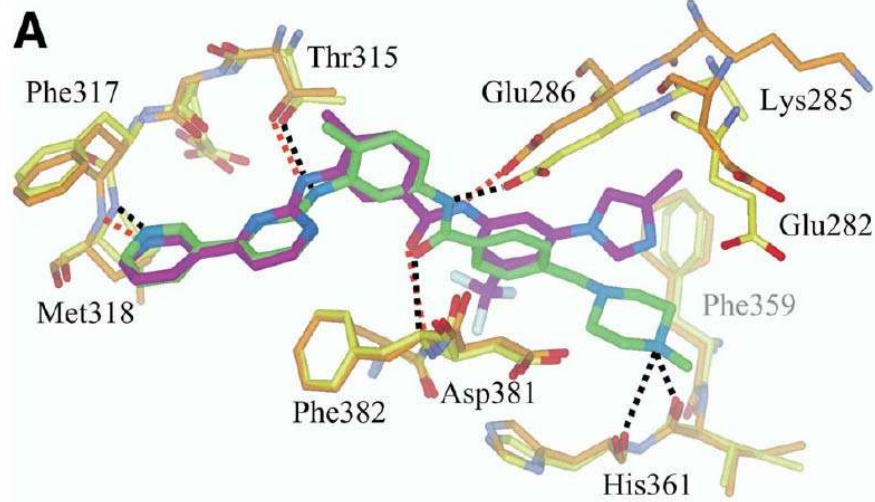
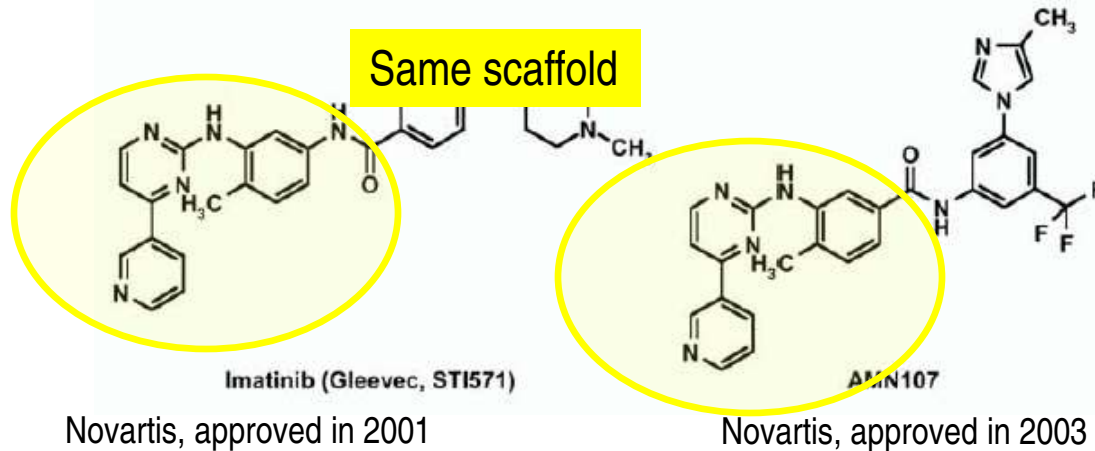
**Imatinib** was developed for chronic myelogenous leukemia (CML), but was also used for gastrointestinal stromal tumors (GISTs) and some other diseases.



$IC_{50} \sim 200 \text{ nM}$

$IC_{50} > 10,000 \text{ nM}$

# Imatinib vs Nilotinib

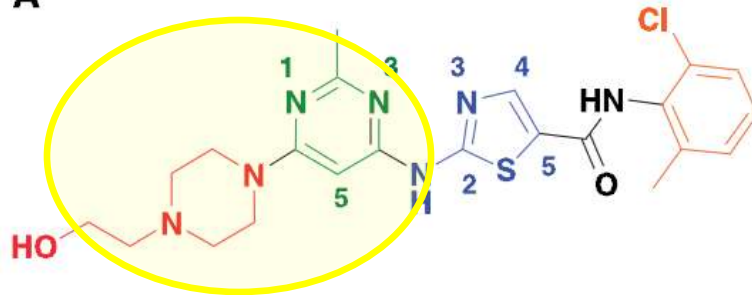


# Dasatinib addresses imatinib resistance mutations, **but** fails with mutant T315I

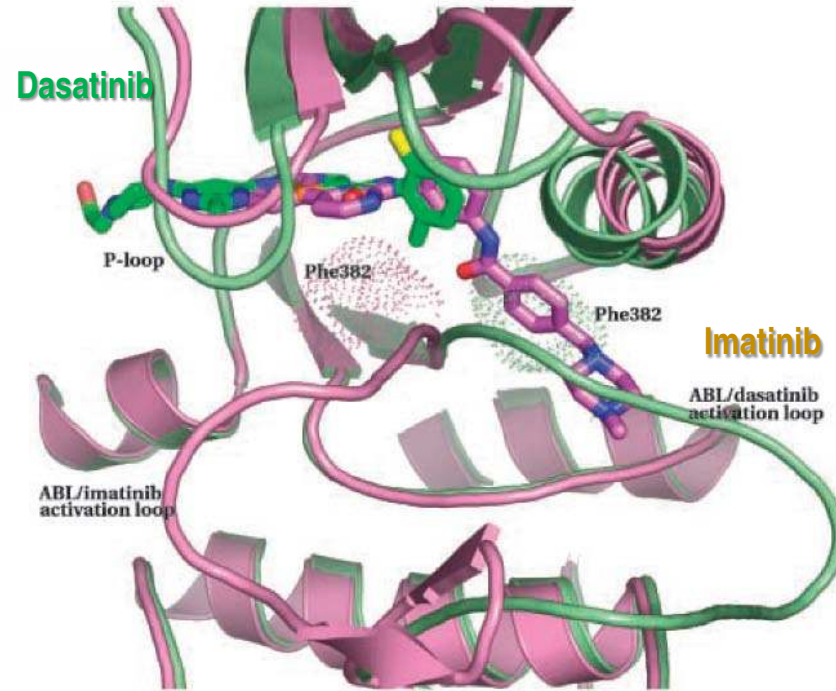
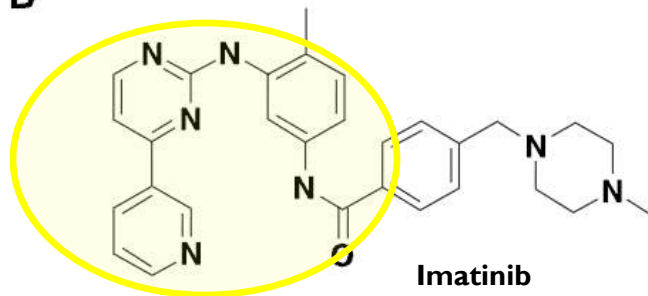
## Dasatinib

Bristol Myers Squibb, approved in 2011

A



B



**Scaffold hopping** via pharmacophore modeling

## ARTICLES

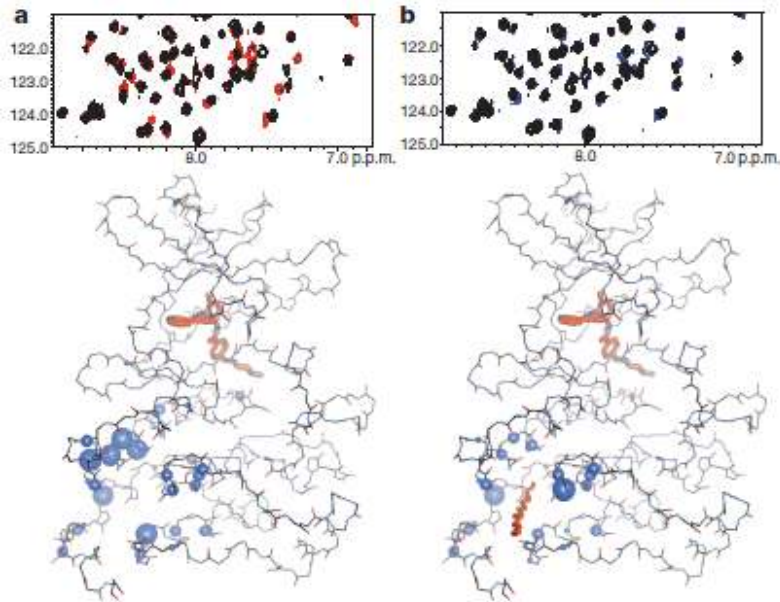
---

# Targeting Bcr–Abl by combining allosteric with ATP-binding-site inhibitors

Jianming Zhang<sup>1\*</sup>, Francisco J. Adrián<sup>2\*</sup>, Wolfgang Jahnke<sup>3</sup>, Sandra W. Cowan-Jacob<sup>3</sup>, Allen G. Li<sup>2</sup>, Roxana E. Iacob<sup>4</sup>, Taobo Sim<sup>1,5</sup>, John Powers<sup>6</sup>, Christine Dierks<sup>2</sup>, Fangxian Sun<sup>2</sup>, Gui-Rong Guo<sup>2</sup>, Qiang Ding<sup>2</sup>, Barun Okram<sup>7</sup>, Yongmun Choi<sup>1</sup>, Amy Wojciechowski<sup>1</sup>, Xianming Deng<sup>1</sup>, Guoxun Liu<sup>2</sup>, Gabriele Fendrich<sup>3</sup>, André Strauss<sup>3</sup>, Navratna Vajpai<sup>8</sup>, Stephan Grzesiek<sup>8</sup>, Tove Tuntland<sup>2</sup>, Yi Liu<sup>2</sup>, Badry Bursulaya<sup>2</sup>, Mohammad Azam<sup>6</sup>, Paul W. Manley<sup>3</sup>, John R. Engen<sup>4</sup>, George Q. Daley<sup>6</sup>, Markus Warmuth<sup>9</sup> & Nathanael S. Gray<sup>1</sup>

**GNF-2 binds to the myristate-binding site of Abl, leads to changes in the structural dynamics of the protein, and thus inhibits allosteric interactions!**

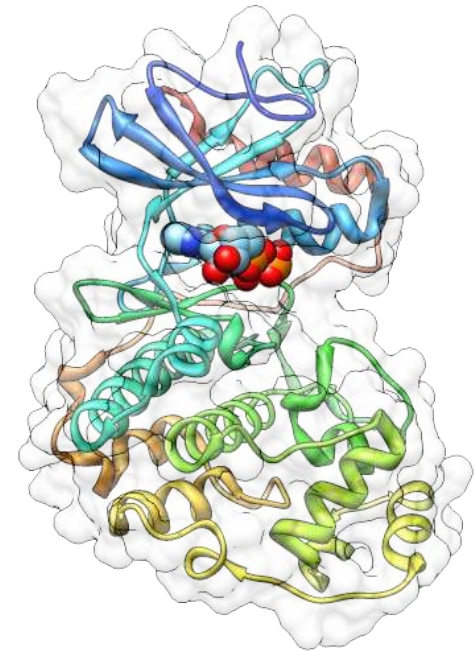
# Polypharmacological strategy: Inhibition of allosteric interaction site in addition to catalytic site



**Evidence for GNF-2 binding to the myristate pocket of Abl.** HSQC spectrum of Abl/Imatinib with (red) and without (black) GNF-2 (top) shows chemical shift changes induced by ligand binding. Mapping of chemical shift changes to structure (PDB 10PK8) identifies the myristate pocket as the GNF-2 binding site. **b**, Same as **a** except myristic acid used instead of GNF-2.

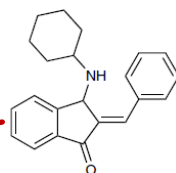
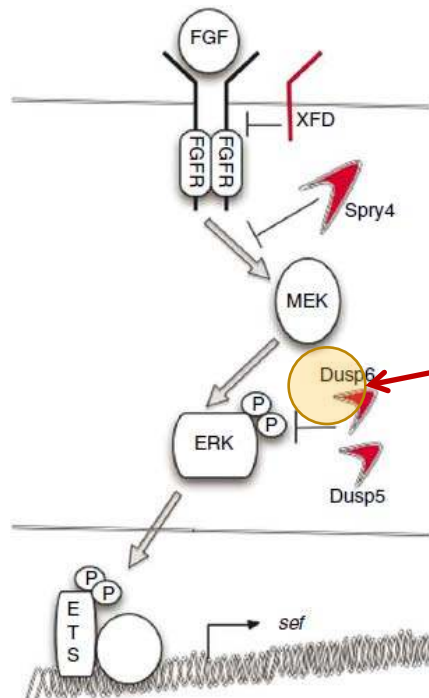
Simultaneously targeting of

- the ATP binding site (by **Gleevec**)
- the myristate pocket (by **GNF-2**)

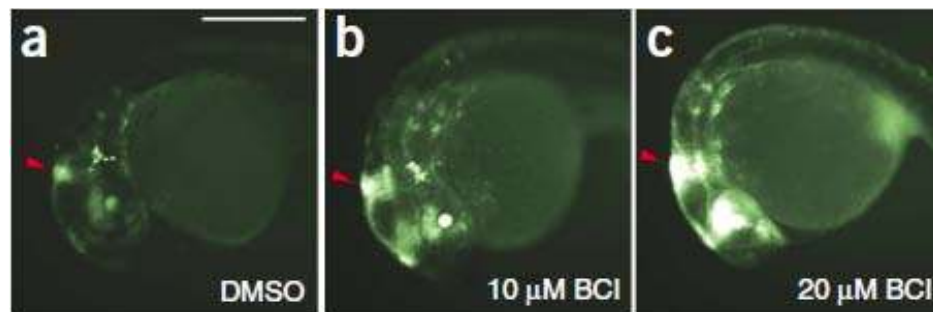


# Zebrafish chemical screening reveals an inhibitor of Dusp6 that expands cardiac cell lineages

Molina G,\* Vogt A,\* Bakan A,\* et al. *Nat Chem Biol*, 2009, 9, 680-7.



**BCI hyperactivates  
FGF signaling**

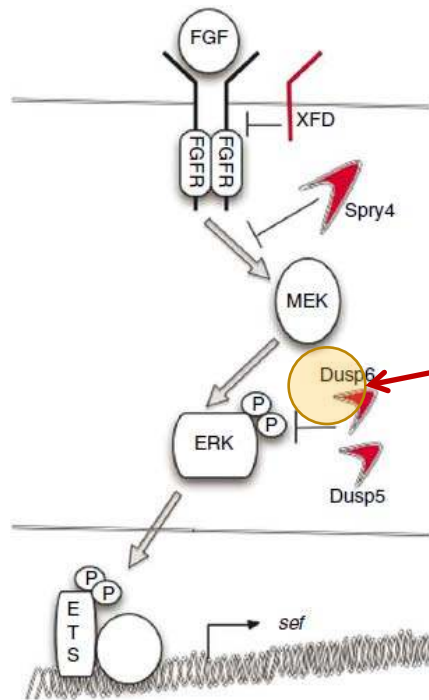


Experiments with transgenic zebrafish embryo showed that FGF signaling is enhanced in the presence of BCI

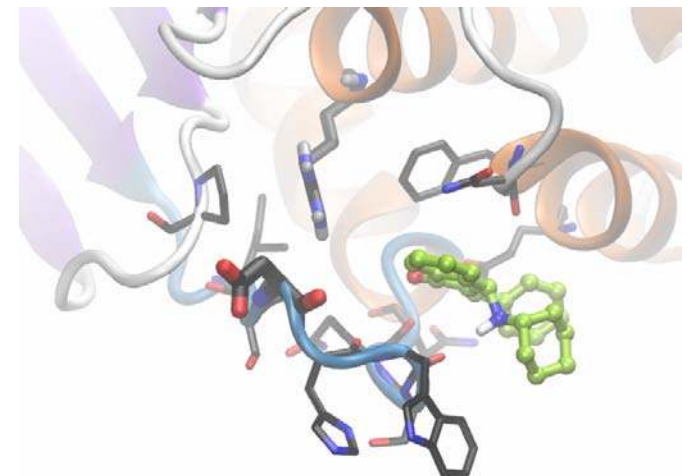
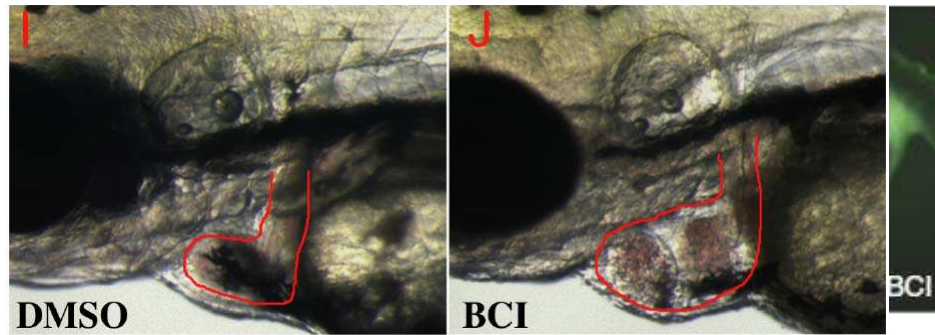
Fibroblast growth factor binding activates the MAPK pathway, leading to cell proliferation, organ development. Dusp6 serves as an attenuator/regulator by inhibiting ERK

# Zebrafish chemical screening reveals an inhibitor of Dusp6 that expands cardiac cell lineages

Molina G,\* Vogt A,\* Bakan A,\* et al. *Nat Chem Biol*, 2009, 9, 680-7.



BCI hyperactivates  
FGF signaling

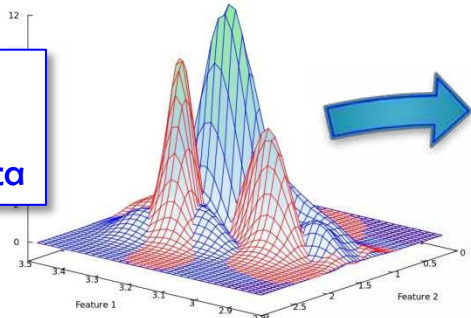


Fibroblast growth factor binding activates the MAPK pathway, leading to cell proliferation, organ development. Dusp6 serves as an attenuator/regulator by inhibiting ERK

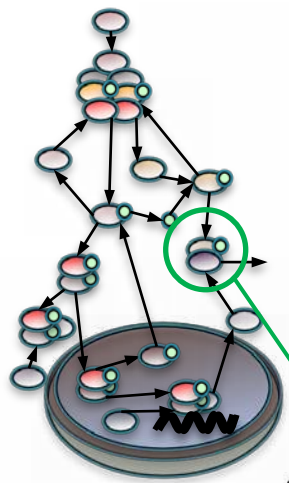
# Quantitative Systems Pharmacology:

## Integrating Quantitative Models with Experimental Data for Drug Discovery

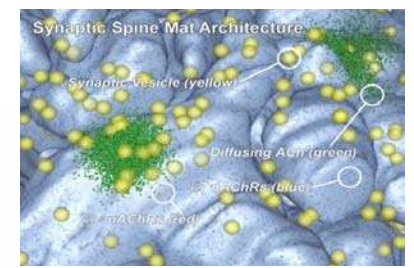
Signals extracted from the data



Information



Refined cellular pathways / processes



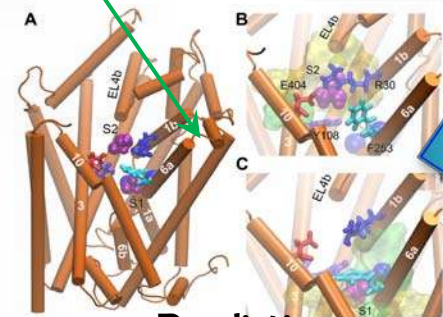
Models

Predicted Drug binding to targets

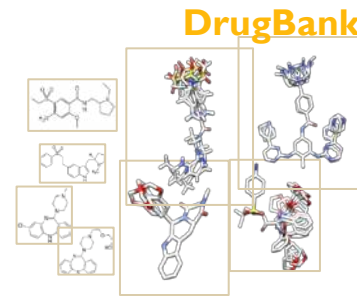
Data

T_1005004	T_1005005	T_1005006	T_1005007	T_1005008	T_1005009	T_1005010
T_4882772	T_4882773	T_4882774	T_4882775	T_4882776	T_4882777	T_4882778
T_9372708	T_9372709	T_9372710	T_9372711	T_9372712	T_9372713	T_9372714
T_6424881	T_6424882	T_6424883	T_6424884	T_6424885	T_6424886	T_6424887
T_6078719	T_6078720	T_6078721	T_6078722	T_6078723	T_6078724	T_6078725
T_1008806	T_1008807	T_1008808	T_1008809	T_1008810	T_1008811	T_1008812
T_102229	T_102230	T_102231	T_102232	T_102233	T_102234	T_102235
T_895127	T_895128	T_895129	T_895130	T_895131	T_895132	T_895133
T_126296	T_126297	T_126298	T_126299	T_126300	T_126301	T_126302
T_1223509	T_1223510	T_1223511	T_1223512	T_1223513	T_1223514	T_1223515
T_100661	T_100662	T_100663	T_100664	T_100665	T_100666	T_100667
T_474789	T_474790	T_474791	T_474792	T_474793	T_474794	T_474795
T_102723	T_102724	T_102725	T_102726	T_102727	T_102728	T_102729
T_17848	T_17849	T_17850	T_17851	T_17852	T_17853	T_17854
T_62641	T_62642	T_62643	T_62644	T_62645	T_62646	T_62647
T_607880	T_607881	T_607882	T_607883	T_607884	T_607885	T_607886
T_89502	T_89503	T_89504	T_89505	T_89506	T_89507	T_89508
T_108211	T_108212	T_108213	T_108214	T_108215	T_108216	T_108217
T_181268	T_181269	T_181270	T_181271	T_181272	T_181273	T_181274
T_88292	T_88293	T_88294	T_88295	T_88296	T_88297	T_88298
T_100206	T_100207	T_100208	T_100209	T_100210	T_100211	T_100212
T_100872	T_100873	T_100874	T_100875	T_100876	T_100877	T_100878
T_12112	T_12113	T_12114	T_12115	T_12116	T_12117	T_12118
T_102217	T_102218	T_102219	T_102220	T_102221	T_102222	T_102223
T_452548	T_452549	T_452550	T_452551	T_452552	T_452553	T_452554
T_481288	T_481289	T_481290	T_481291	T_481292	T_481293	T_481294
T_104381	T_104382	T_104383	T_104384	T_104385	T_104386	T_104387

Data

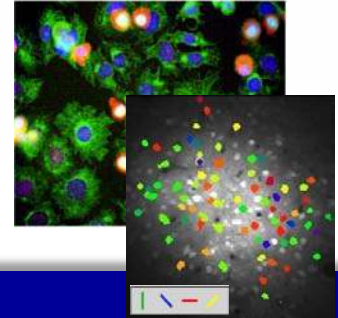


Predictions



High-Content Screen  
Targeted Libraries

Measurements of biological functions



3D or 4D images

Experimental testing

Clinical Trials